IRAQI JOURNAL OF MATERIALS
Volume (4) Issue (3) July-September 2025, pp. 139-144

Surface Quality of Metallic Microstructures Produced by Pulsed Laser-Based Manufacturing

Saad M. Hameed, Fuad Y. Khallaf

Department of Mechanical Engineering, College of Engineering, University of Tikrit, Tikrit, IRAQ

Abstract
In this work, material removal process was performed using pulsed Nd:YAG laser of 60kW peak power to manufacture microstructures from Inconel samples at micrometer dimensions for micro-stamping and micro-embossing on metals. Effects of laser power density, overlap between laser pulses and processing velocity on the quality of the machined surfaces were determined. The surface roughness was decreased to about 1 micron as the velocity of laser beam was increased to 300 mm/s.

Keywords: Laser-based manufacturing; Material removal; Microstructure; Inconel alloys
Received: 11 April 2025; **Revised:** 18 June 2025; **Accepted:** 25 June 2025; **Published:** 1 July 2025

1. Introduction

With the recent progress of microelectromechanical systems, interest in the fabrication of microstructures using different methods and materials is increasing. Titanium and Inconel are excellent materials exhibiting high corrosion resistance, strength-to-weight ratio, low modulus of elasticity [1-3]. Furthermore, they are biocompatible materials employed for medical implants. Biomedical microdevices, microgripper or sensors are required to meet the biocompatibility and safety considerations if installation in living body is considered [4-5]. Laser machining is a promising technique to fabricate metallic microstructures because no mechanical contact exists [6-8]. Direct laser machining, however, has drawbacks due to high thermal load that may lead to thermal deformation of microstructures or poor surface quality by melting and droplet formation [9-11]. The material removal is related to the total absorbed energy, and it is the thermo-physical behavior which is most complicated, involving particle trajectories and flow of both liquids and solids [12-14].

Requiring fast and flexible methods to manufacture microstructures and parts at decreased costs, needs for micro-tools have increased in too special way [15-17]. The needed microstructures have some requirements must be satisfied such as very small dimensions (<100µm), high aspect ratio (>1:20) and too small roughness of surfaces (<1µm). As the tools used for stamping, embossing, injection molding and other similar applications must be made of hard metals as they should be weariless. The electric discharge machining can be considered as an available alternative, but the costs of microstructured electrodes are high [9]. This problem can be solved by using Nd:YAG laser to manufacture microstructures. The advantages of laser micromachining include small heat affected zone (HAZ), control over machining depth, rapid throughout and accomplishment of machining at any time during or after processing [18-20].

The Nd:YAG laser is employed in a direct writing method with radiation and hard metals can be structured with Nd:YAG laser method since it has no material restrictions. Additionally, the development of high-quality diode-pumped Nd:YAG lasers opened new fields in machining with higher harmonic generation, high beam quality, short laser pulse and high precision positioning tables. All these specifications improve quality of the produced microstructures [21-23]. Usually, production of micro-parts and micro-tools by Nd:YAG laser removal requires so low technical effort to be achieved [24-26].

In this paper, using of pulsed Nd:YAG laser for material removal process to manufacture microstructures from Inconel-600 samples at micrometer dimensions for micro-stamping and micro-embossing on metals is described. Effects of different parameters, such as power density, overlap of laser pulses and processing velocity, on the quality of the machined surfaces will be introduced.

2. Experiment

An important parameter for the laser beam removal with a pulsed Nd:YAG laser is the overlap between laser pulses. This parameter determines the material removal depth per laser pulse, which can

be higher than the depth of a single laser pulse, and the quality of the worked surface. Subsequent overlapping laser-pulses deposit some of the newly ejected material back into previously machined cavities. The nature of the resultant kerf depends on the percentage overlap and the aspect (depth-to-width) ratio of the kerf. In Fig. (1), the relation between the overlap and the single laser pulses is shown. The definition of the overlap (*O*) is [27]:

$$O = (1 - \frac{m}{d_w}) \times 100\% \quad (1)$$

where *m* is the distance between two laser pulses, and d_w is effecting working diameter of the laser beam

Experiments show that with overlap of less than 60%, the kerf remains clean and material flow is small. For larger overlap, the kerf is substantially closed by resolidified material [8]. The effecting working diameter (d_w) needs not to be equal to the focus diameter. Definition of the focus diameter does not depend on the maximum of the power density of the laser beam, but on the power density distribution [28].

One criteria of the quality of a microstructure is the roughness and the structure of the machined surface. For this reason Inconel samples was examined, which can be used as stamping and embossing tools.

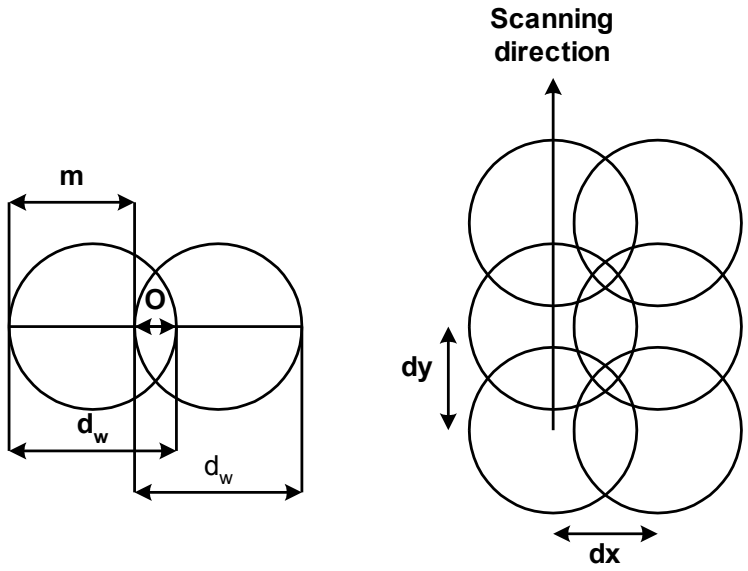

Fig. (1) Overlap principle of laser pulses

The laser system is a 300μs duration Nd:YAG laser operating at 1064nm and the Gaussian mode (TEM_{00}), a high-energy stability and a beam divergence of about 1.5mrad. The focus diameter is 50μm with a quartz lens of 2.54cm focal length. The peak power obtained is about 60kW and average power delivered is 10W at 1064nm. Samples processed are 2cm-thickness Inconel-600. Mechanical and physical properties of this alloy are characterized by 225Hv hardness, 1665K melting temperature and $7.1 \times 10^{-6} m^2/s$ thermal diffusivity at 273K.

Manual moving table was used for the coarse movement as the technique used in this work requires too precise positioning, so, a computerized step-motor *xyz*-positioning stage was used onto the manual table for fine movement. A QuickBasic 3.0 software was used for controlling the motion of the xyz-stage, which has high dynamic and precise linear drivers. The resolution of the position is 1μm, the positioning accuracy is 10 μm and the maximum velocity (sample velocity) is 50mm/s. Laser beam was guided to the focusing lens (L) by mirror (M1) through the beam splitter (BS), as shown in Fig. (2). The beam splitter was used to feed the vision system (camera) accessorized with laser system. The focusing lens was connected with the *z*-axis, while the workpiece was fixed on the *x*-axis and *y*-axis. The position of the focus of laser beam relative to the workpiece can be adjusted with the *z*-axis.

3. Results and Discussion

At an overlap of 0%, the average depth of removal per laser pulse is equal to the removal depth of a single laser pulse. The average removal depth per laser pulse, hence the thickness of a single slice,

increases as the overlap increases. A single laser pulse may cause to its incidence position on the sample to melt, therefore, when overlap is high, a part of processed region will receive much more energy. As a result, removal depth increases. However, too higher overlap may cause thermal damage to the material since more overlap means higher power density, i.e., more thermal effect on same localized area. Thermal effect has induced changes in the properties of processed region since most mechanical and physical properties of metals are temperature-dependent. Figure (3) shows an SEM image of a hole drilled in the surface of Inconel-600 sample with 100 μm diameter.

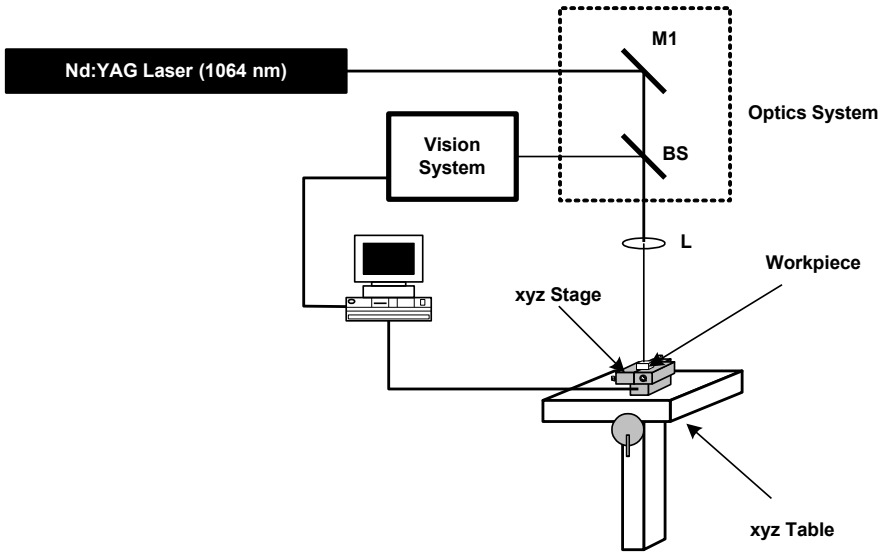

Fig. (2) Experimental set-up used in this work

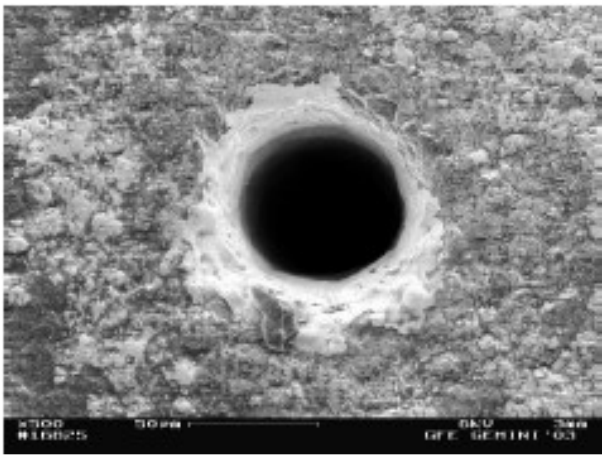

Fig. (3) SEM image of a hole drilled in the surface of Inconel-600 sample with 100 μm diameter

Figure (4) shows variation of the roughness (R_a) of the surface machined as a function to the overlap of laser pulses in *x*- and *y*-direction. Both roughness components (R_x and R_y) show an overall increasing trend as the overlap increases from around 10% to nearly 100%, highlighting the cumulative effect of multiple laser pulses on material morphology. At lower overlaps (below ~40%), the roughness rises quickly, suggesting significant initial texturing and surface modification. Beyond this region, the growth becomes more gradual, though R_x continues to rise more steeply than R_y at higher overlaps, exceeding 5 microns at full overlap. This divergence indicates anisotropic effects in the scanning process, possibly due to pulse energy distribution, heat accumulation, or material response differences along orthogonal directions. The error bars show that variability is more pronounced at higher overlaps, which could be attributed to unstable melting, redeposition, or microstructural heterogeneity. Critically, the chart underscores that higher pulse overlap enhances surface roughness, which could be beneficial for applications requiring textured surfaces (e.g., adhesion) but detrimental for optical or electronic

 ISSN (print) 2958-8960 (online) 3006-6042 Printed in IRAQ

applications demanding smoothness. The fitted curves confirm nonlinear behavior, likely influenced by complex thermomechanical and photothermal interactions, making process optimization essential to balance functional surface properties. Roughness increases because the increasing overlap has concentrated laser power on the overlapping region. Liquid-phase molten moves toward expanding direction due to thermodynamics of fluids. As it starts to resolidify, non-uniform distribution of mass results. Depth of removal material increases as power density does, hence surface will be distorted more than before which means more roughness as in Fig. (5). This figure demonstrates the effect of increasing power density on surface roughness during laser processing. As power density rises from nearly 0 to around 4×10^5 W/cm², roughness increases nonlinearly from about 1.5 to over 5 microns. The curve suggests a quadratic or exponential relationship, highlighting how higher power intensifies local melting, vaporization, and redeposition, leading to more pronounced texturing and peak-valley formation. The data points also show modest variability, as reflected by the error bars, which become slightly larger at higher power densities—likely due to instability in melt dynamics or material ejection. Overall, the plot confirms that controlling power density is crucial for tuning surface roughness and final texture.

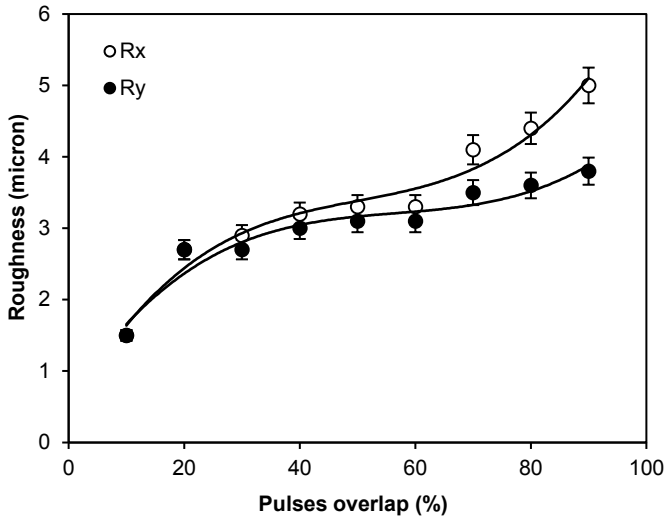

Fig. (4) Effect of overlap between laser pulses on the roughness of the machined surface in *x*- (R_x) and *y*-directions (R_y)

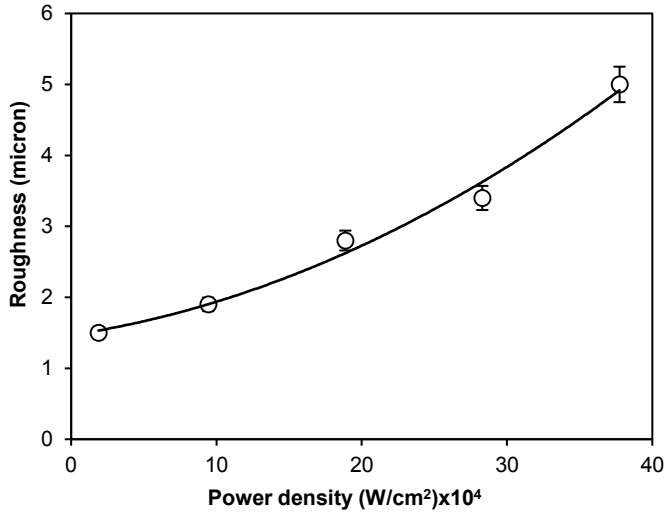

Fig. (5) Effect of laser power density on the roughness of the machined surface (R_a)

Figure (6) illustrates the inverse relationship between scanning velocity and surface roughness during laser processing. As can be seen from this figure, roughness decreases with increasing velocity of laser beam. The surface roughness was decreased from 1.2 to reach about 1 μm as the velocity of laser beam was increased from 50 to 300 mm/s, respectively, therefore, laser beam velocity must be

carefully determined. Low velocity allows energy per unit area to accumulate leading to higher power density. High velocity prevents pulses to overlap and reduces power received by processed region. As a result, reduced roughness would be achieved. At very low velocities (~10 mm/s), the roughness peaks above 5 µm due to prolonged laser–material interaction, causing excessive melting and resolidification irregularities. As velocity increases to around 50–100 mm/s, roughness rapidly drops below 1.5 µm, indicating more controlled energy input and smoother solidification. Beyond 100 mm/s, further increases in velocity yield only marginal improvement, stabilizing roughness near 1 µm. This trend shows that optimizing scanning speed is critical: excessively slow speeds

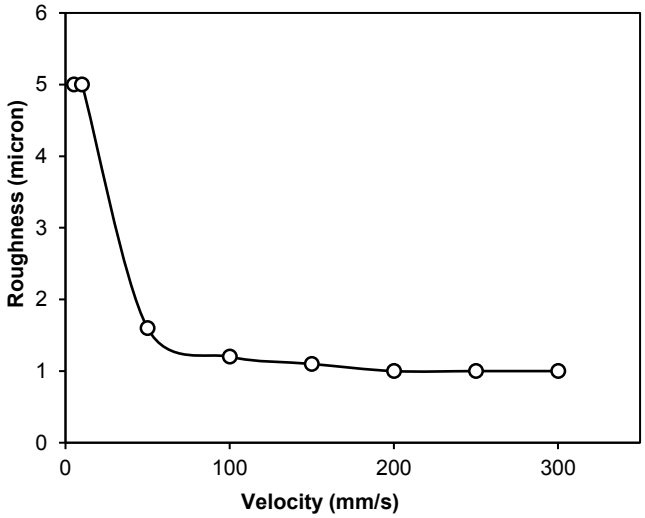

Fig. (6) Effect of laser beam velocity on the roughness of the machined surface (R_a)

4. Conclusions

Forming microstructures with Nd:YAG laser expands the range of manufacturing techniques for the production of micro-tools. The main advantages of this technology are the variety of materials, flexibility and short cycle from the control software to the machining system. This technology can reduce manufacturing costs of micro-parts. Roughness can be decreased as the overlap of laser pulses decreases and it is recommended to work at the optimum value of overlap that permits to obtain optimum removal depth, hence optimum thickness of a single slice. The basic and complex shapes are possible to produce micro-tools for stamping and embossing of metal parts.

References

[1] J. Dutta Majumdar and I. Manna, "Laser Material Processing", *Sadhana*, 28 (3-4) (2003) 495-562.
[2] R. Lawes, A. Holmes and F. Goodall, *Microsystem Technol.*, 3 (1996) 17-19.
[3] W. Juan and S. Pang, *J. Vac. Sci. Technol. B*, 12(1) (1994) 422-426.
[4] H. Yu, B. Li and X. Zhang, "Direct Scanning Laser Writing of 3D Multulayer Microstructures", Department of Manufacturing Engineering, Boston University, 2002, *private communications*.
[5] S. Jeong, Y. Shin and S. Son, "Laser-Induced Thermochemical Wet Etching of Titanium Foil for Fabrication of Microstructures", Department of Mechatronics, KIST (Korea), 2001, *private communications*.
[6] Y. Yashkir, "Laser Micromachining with Passively Q-switched Intracavity Harmonic Generator", Phot. Res. Ontario (Canada), 2000, *private communications*.
[7] W. Zhang and Y. L. Yao, "Micro Scale Laser Shock Processing of Metallic Components", Department of Mechanical Engineering, Columbia Univ. (NY), 2002, *private communications*.
[8] M. Cohen, R. Kaplan and E. Arthurs, *Proc. IEEE,* 70(6) (1982) 545-554.
[9] Gillner, *Proc. of the MicroEngineering'96*, Stuttgart (1996) 51-55.
[10] L. Migliore, "**Laser Materials Processing**", Marcel Dekker (NY) (1996) 141-142.
[11] W.W. Duley, "**CO_2 Lasers, Effects and Applications**", Academic Press (NY), (1976) 273.
[12] N. Tabata, S. Yagi and M. Hishii, *J. Mater. Process. Tech.,* 62(4) (1996) 309-314.
[13] H. Tonshoff et al., *Proc. SPIE,* 229 (1997) 183-193.
[14] R. Jandeleit et al. *J. Appl. Phys.,* A36 (1996) 117-121.
[15] Y.-C. Tsai et al., *J. Chromatography A*, 1111 (2006) 267–271.
[16] E.R. Choban et al., *J. Power Sources*, 128 (2004) 54-60.
[17] A. Bazylak, D. Sinton, and N. Djilali, *J. Power Sources*, 143 (2005) 57-66.
[18] S.A.Mousavi Shaegh, N.-T. Nguyen, and S.H. Chan, *Int. J. Hydro. Energy*, 36(9) (2011) 5675-5694.
[19] T.Z. Jubery et al., *Biomicrofluid.*, 6 (2012) 016503.
[20] V. Dolnik, S. Liu, and S. Jovanovich, Electrophoresis, 21 (2000) 41-54.

[21] B. Darling, “MicroFabrication: Photolithography”, presentation EE-527, Dept. of Elect. Eng., University of Washington (2015).
[22] B. Jung, R. Bharadwaj, and J.G. Santiago, *Anal. Chem.*, 78(7) (2006) 2319–2327.
[23] M.R. Mohamadi et al., *Anal. Chem.*, 79 (2007) 3667-3672.
[24] J. Wang et al., *Electrophoresis*, 30 (2009) 3250-3256.
[25] D. Bottenus et al., *Lab Chip*, 11(22) (2011) 3793-3801.
[26] D. Bottenus et al., *Lab Chip*, 11(5) (2011) 890-898.
[27] M.R. Hossan et al., J. Colloid Interface Sci., 394 (2013) 619-629.
[28] A Guide to Polyacrylamide Gel Electrophoresis and Detection, Ch. 1, Bulletin 6040 Rev B, Bio-Rad Laboratories, Inc. (2015) p. 3.

 ISSN (print) 2958-8960 (online) 3006-6042 Printed in IRAQ